7

Location and severity of aortic valve calcium and implications for aortic regurgitation after transcatheter aortic valve implantation

Ewe SH, Ng AC, Schuijf JD, van der Kley F, Colli A, Palmen M, de Weger A, Marsan NA, Holman ER, de Roos A, Schalij MJ, Bax JJ, Delgado V.

Am J Cardiol. 2011 Nov 15;108(10):1470-7.

Location and Severity of Aortic Valve Calcium and Implications for Aortic Regurgitation After Transcatheter Aortic Valve Implantation

See Hooi Ewe, MBBS[a,b], Arnold C.T. Ng, MBBS, PhD[a], Joanne D. Schuijf, PhD[a], Frank van der Kley, MD[a], Andrea Colli, MD[c], Meindert Palmen, MD, PhD[a], Arend de Weger, MD[a], Nina Ajmone Marsan, MD[a], Eduard R. Holman, MD, PhD[a], Albert de Roos, MD, PhD[d], Martin J. Schalij, MD, PhD[a], Jeroen J. Bax, MD, PhD[a], and Victoria Delgado, MD, PhD[a,*]

Location of aortic valve calcium (AVC) can be better visualized on contrast-enhanced multidetector row computed tomography. The present evaluation examined whether AVC severity and its location could influence paravalvular aortic regurgitation (AR) after transcatheter aortic valve implantation. A total of 79 patients (age 80 ± 7 years, 49% men) with preprocedural multidetector row computed tomography were included. Volumetric AVC quantification and its location were assessed. Transesophageal echocardiography was performed to assess the presence and site of AR after transcatheter aortic valve implantation. Receiver operating characteristic curves were generated to evaluate the usefulness of AVC in determining paravalvular AR at a specific site. Postprocedural AR of grade 1 or more was observed in 63 patients. In most patients (n = 56, 71%), AR was of paravalvular origin. Calcium at the aortic wall of each valve cusp had the largest area under the curve (0.93, p <0.001) in predicting paravalvular AR at the aortic wall site compared to calcium at the valvular edge or body (area under the curve 0.58 and 0.67, respectively). Calcium at the valvular commissure was better than calcium at the valvular edge (area under the curve 0.94 vs 0.71) in predicting paravavular AR originating from the corresponding commissure. In conclusion, contrast-enhanced multidetector row computed tomography can be performed to quantify AVC. Both AVC severity and its exact location are important in determining paravalvular AR after transcatheter aortic valve implantation. **(Am J Cardiol 2011;108:1470–1477)**

Multidetector row computed tomography (MDCT) allows visualization of the precise location of aortic valve calcium (AVC).[1,2] The present evaluation aimed to determine whether the severity and location of AVC would influence the occurrence and location of paravalvular aortic regurgitation (AR) after transcatheter aortic valve implantation (TAVI).

Methods

A total of 79 patients with symptomatic, severe aortic stenosis (AS) who underwent MDCT before TAVI were included. The patients with bicuspid aortic valves or failing bioprosthetic valves (valve-in-valve) and those who did not eventually receive TAVI were excluded. An Edwards-Sapien device (Edwards Lifesciences, Irvine, California) was implanted in all patients using either the transfemoral or transapical approach.

According to the institutional protocol, all patients underwent a detailed clinical evaluation and preoperative transthoracic echocardiography to examine AS severity, valve morphology, and left ventricular (LV) function. Preoperative multidetector row computed tomographic scans were also performed to assess the aortic valve and aortic root and the extent and distribution of AVC.[3] Transesophageal echocardiography (TEE) was performed intraprocedurally and to evaluate the function of the prosthesis immediately after valve deployment, including the assessment of the AR location, if present.[3] The clinical, echocardiographic, and multidetector row computed tomographic data were prospectively collected in an electronic patient dossier (EPD Vision, version 8.3.3.6, Leiden, The Netherlands) and retrospectively analyzed.

The patients underwent imaging preoperatively using a commercially available ultrasound system (Vingmed Vivid-7, General Electric Vingmed, Horten, Norway). A complete 2-dimensional, color, pulsed, and continuous-wave Doppler echocardiographic examination was performed.[3–5] The LV end-diastolic volume and end-systolic volume were measured (indexed to the body surface area), and the LV ejection fraction was derived using biplane Simpson's method.[3,4] Aortic valve morphology

[a]Department of Cardiology and Cardiothoracic Surgery, Leiden University Medical Center, Leiden, The Netherlands; [b]Department of Cardiology, National Heart Centre, Singapore, Singapore; [c]Department of Cardiothoracic Surgery, Hospital Germans Trias i Pujol, Badalona, Spain; and [d]Department of Radiology, Leiden University Medical Center, Leiden, The Netherlands. Manuscript received May 25, 2011; manuscript received and accepted July 5, 2011.

*Corresponding author: Tel: (+31) 7-1526-2020; fax: (+31) 7-1526-6809.

E-mail address: v.delgado@lumc.nl (V. Delgado).

0002-9149/11/$ – see front matter
doi:10.1016/j.amjcard.2011.07.007

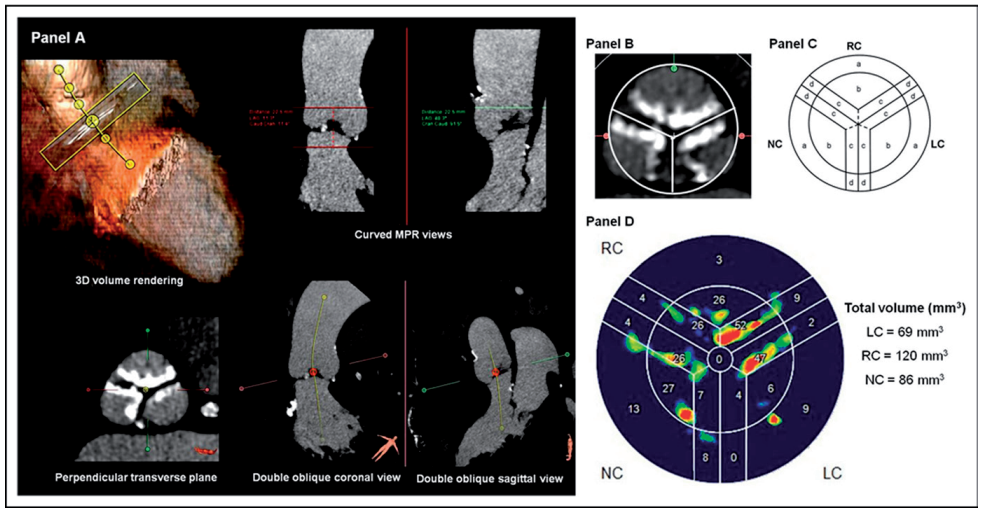

Figure 1. *(A)* Automatic segmentation of aortic root with center line by dedicated software (3mensio Valve, version 4.1.sp2, 3mensio Medical Imaging BV). By moving the 2 orthogonal MPR planes and the third perpendicular transverse plane, manual adjustment of the center line is possible. Next, by moving the transverse plane along the center line, the region of interest for quantification of calcium is defined manually using the help of the curved MPR view (from the level of the LV outflow tract proximally to the level just below the coronary ostia distally). From the transverse MPR view *(B)*, the aortic valve is automatically divided into 3 cusps and manual adjustment of the divisions (arms) between the cusps is possible. The software will automatically detect areas of calcium according to the predetermined threshold set by the user and provide their locations and corresponding volumetric measurements *(C, D)*. *(D)* Example shown. *(C)* Six locations of calcium can be identified on each cusp. a = along aortic wall; b = valvular body; c = valvular edge; d = commissure; LC = left coronary cusp; NC = noncoronary cusp; RC = right coronary cusp.

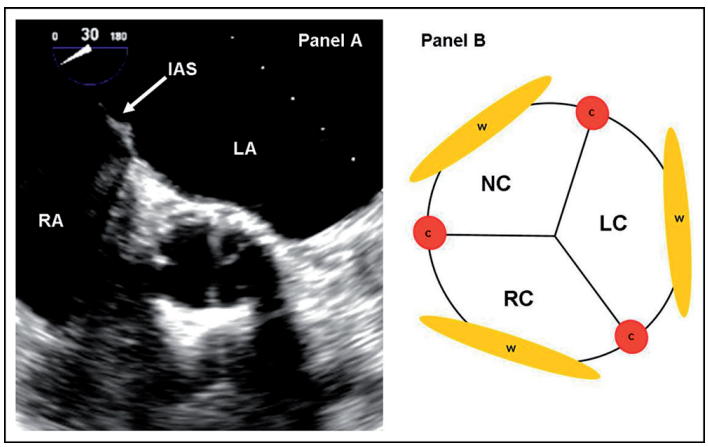

Figure 2. Identification of sites of AR after TAVI using TEE. Short-axis view, at level of proximal (ventricular) end of prosthesis, permits visualization of origin of paravalvular regurgitation. Interatrial septum helps to identify the noncoronary cusp *(A)*. *(B)* Six possible sites of paravalvular regurgitation. c = commissure site; IAS = interatrial septum; LA = left atrium; LC = left coronary cusp; NC = noncoronary cusp; RA = right atrium; RC = right coronary cusp; w = aortic wall site.

was evaluated using the parasternal short-axis view, and the valve area was determined by the continuity equation.[6] The peak and mean transaortic pressure gradients were calculated.[6] AR was assessed using color Doppler after optimizing the gain and Nyquist limit, and its severity was assessed.[7]

Table 1
Baseline clinical characteristics before transcatheter aortic valve implantation (TAVI)

Variable	All (n = 79)	Paravalvular AR (n = 56)	No Paravalvular AR (n = 23)	p Value
Men	39 (49%)	30 (54%)	9 (39%)	0.32
Age (years)	80 ± 7	80 ± 7	81 ± 6	0.54
Body mass index (kg/m^2)	25.5 ± 4.6	24.9 ± 3.0	26.8 ± 7.0	0.22
Body surface area (m^2)	1.82 ± 0.19	1.84 ± 0.17	1.78 ± 0.22	0.18
Logistic EuroSCORE (%)	23 ± 13	23 ± 12	21 ± 14	0.44
Hypertension	46 (58%)	32 (57%)	14 (61%)	0.81
Hypercholesterolemia	33 (42%)	21 (38%)	12 (52%)	0.32
Diabetes mellitus	22 (28%)	18 (32%)	4 (17%)	0.27
Peripheral vascular disease	23 (29%)	16 (29%)	7 (30%)	1.00
Previous myocardial infarction	19 (24%)	13 (23%)	6 (26%)	0.78
Previous coronary artery bypass	31 (39%)	24 (43%)	7 (30%)	0.45

Continuous data are presented as mean ± SD and categorical data as n (%).
EuroSCORE = European System for Cardiac Operative Risk Evaluation.

Table 2
Baseline echocardiographic characteristics before transcatheter aortic valve implantation (TAVI)

Variable	All (n = 79)	Paravalvular AR (n = 56)	No Paravalvular AR (n = 23)	p Value
Left ventricular end-diastolic volume (ml/m^2)	67 ± 26	70 ± 27	58 ± 21	0.06
Left ventricular end-systolic volume (ml/m^2)	35 ± 23	37 ± 24	30 ± 22	0.18
Left ventricular ejection fraction (%)	52 ± 12	51 ± 14	54 ± 15	0.39
Mean transaortic gradient (mm Hg)	40 ± 14	38 ± 16	38 ± 12	0.94
Peak transaortic gradient (mm Hg)	61 ± 22	62 ± 24	60 ± 17	0.79
Aortic valve area (cm^2)	0.74 ± 0.18	0.76 ± 0.18	0.69 ± 0.18	0.15
Aortic regurgitation				
None	18 (23%)	11 (20%)	7 (30%)	0.61
Mild	48 (61%)	35 (63%)	13 (57%)	
Moderate	13 (16%)	10 (17%)	3 (13%)	
Severe	0	0	0	

Continuous data are presented as mean ± SD and categorical data as n (%).

All patients underwent preoperative evaluation of the aortic valve and aortic root with either a 64-detector or 320-detector row computed tomography scanner (Aquilion 64 and Aquilion ONE, respectively, Toshiba Medical Systems, Otawara, Japan). The acquisition protocols of the multidetector row computed tomographic data for the Aquilion 64 and Aquilion ONE have been previously described.[8] Before each scan, the patients with a heart rate greater than the threshold of 65 beats/min received oral β blockers (50 to 100 mg metoprolol), unless contraindicated. All multidetector row computed tomographic scans were acquired during midinspiratory breath-hold. To synchronize the arrival of the contrast media, bolus arrival was detected using a real-time bolus tracking technique with a threshold of +180 Hounsfield units. All the multidetector row computed tomographic data sets were recorded and stored for postprocessing.

The assessment of AVC was performed using the diastolic images, at 75% of the RR interval of the contrast-enhanced multidetector row computed tomographic scans.[8] The region of interest on the aortic valve, from which AVC quantification was performed, included (from proximal to distal) the LV outflow tract, aortic annulus, valvular cusps, and the adjacent aortic walls (until the level before the appearance of coronary ostium distally on the double oblique transverse view). Mitral annular calcification and atherosclerosis of the upper aortic root (distal to the coronary ostia level) were excluded from AVC quantification. AVC was measured quantitatively using a novel automated data postprocessing software (3mensio Valve, version 4.1.sp2, 3mensio Medical Imaging BV, Bilthoven, The Netherlands). An empiric threshold of ≥800 Hounsfield units was used to detect areas of calcium in the region of interest, because the luminal contrast enhancement ranged from 250 to 760 Hounsfield units. As previously reported,[9,10] calcium quantification using the Agatston score requires a nonlinear weighting factor in its derivation and thus has been shown to exhibit greater variability than the volumetric quantification of calcium. Accordingly, we quantified AVC in cubic millimeters instead of using the Agatston score.

First, from the 3 multiplanar reformation (MPR) planes and the 3-dimensional reconstruction, the aortic root was automatically segmented and a center line crossing the aortic lumen displayed (Figure 1). The center line and the perpendicular MPR plane were manually adjusted to improve accuracy using the aortic cusps as a guide, whereby the 2 orthogonal MPR planes would bisect the long axis of the aortic cusps in parallel, and a third perpendicular transverse plane would bisect the 3 aortic cusps. The true trans-

Table 3
Baseline multidetector row computed tomographic measurements of total volume of aortic valve calcium (AVC) and its respective location at aortic cusp in patients with and without paravalvular aortic regurgitation (AR)

Variable	Paravalvular AR (n = 56)	No Paravalvular AR (n = 23)	p Value
Total calcium volume (mm^3)	367.1 ± 35.9	222.3 ± 43.3	0.023*
Calcium on left cusp (mm^3)	105.4 ± 14.3	40.6 ± 10.5	0.007*
Calcium on right cusp (mm^3)	102.2 ± 13.1	61.9 ± 77.3	0.082
Calcium on noncoronary cusp (mm^3)	160.2 ± 16.6	95.9 ± 19.3	0.028*
Calcium on wall of left cusp (mm^3)	28.6 ± 3.5	10.8 ± 5.4	0.008*
Calcium on wall of right cusp (mm^3)	25.0 ± 4.7	11.5 ± 7.1	0.12
Calcium on wall of noncoronary cusp (mm^3)	46.1 ± 6.1	19.0 ± 11.9	0.029*
Calcium on edge of left cusp (mm^3)	33.3 ± 5.9	15.6 ± 5.6	0.076
Calcium on edge of right cusp (mm^3)	37.7 ± 5.7	25.6 ± 5.8	0.21
Calcium on edge of noncoronary cusp (mm^3)	42.7 ± 7.0	33.0 ± 7.5	0.42
Calcium on body of left cusp (mm^3)	29.2 ± 6.1	10.6 ± 2.9	0.060
Calcium on body of right cusp (mm^3)	23.8 ± 5.0	13.2 ± 4.5	0.20
Calcium on body of noncoronary cusp (mm^3)	54.7 ± 7.3	34.8 ± 7.8	0.11
Calcium on left–right commissure (mm^3)	13.4 ± 2.2	2.8 ± 1.1	0.003*
Calcium on left–noncoronary commissure (mm^3)	9.8 ± 2.7	1.2 ± 0.6	0.050
Calcium on right–noncoronary commissure (mm^3)	12.5 ± 2.5	6.1 ± 1.8	0.11
Calcium on left–right edge (mm^3)	36.1 ± 6.6	20.0 ± 5.9	0.15
Calcium on left–noncoronary edge (mm^3)	40.5 ± 6.4	23.3 ± 4.0	0.098
Calcium on right–noncoronary edge (mm^3)	37.2 ± 5.7	30.8 ± 8.4	0.54

Continuous data are presented as mean ± SEM.

Table 4
Prevalence of paravalvular regurgitation on transesophageal echocardiograms after transcatheter aortic valve implantation (TAVI)

Variable	Paravalvular AR		
	None (n = 23)	Grade 1 (n = 47)	Grade 2 (n = 9)
Wall of left cusp	51 (10.8%)	25 (5.3%)	3 (0.6%)
Wall of right cusp	61 (12.9%)	16 (3.4%)	2 (0.4%)
Wall of noncoronary cusp	43 (9.1%)	33 (7.0%)	3 (0.6%)
Left–right commissure	70 (14.8%)	9 (1.9%)	0
Left–noncoronary commissure	74 (15.6%)	3 (0.6%)	2 (0.4%)
Right–noncoronary commissure	73 (15.4%)	6 (1.2%)	0

Data are presented as absolute number of transesophageal echocardiographic sites with or without paravalvular AR (expressed as percentage of 474 potential sites in total); 6 sites in each patient for a total of 474 sites in 79 patients.

verse plane should be seen to bisect the aortic cusps equally, permitting visualization of the insertion points of all 3 aortic cusps at the level of the aortic annulus. Subsequently, by adjusting the level of the transverse plane, the center line should sit in the center of the 3 aortic cusps at the level of aortic sinus (Figure 1). Next, the software automatically displayed the true short axis of the aortic valve in the transverse MPR view (Figure 1). Then, the additional 2 orthogonal curved MPR views were used to define the region of interest (from the LV outflow tract level to the level before the appearance of the coronary ostium). The software then automatically provided AVC quantification and the exact location of calcium (Figure 1). Six locations of calcium were identified on each cusp (Figure 1), and the respective AVC could be quantified in cubic millimeters (Figure 1).

Immediately after prosthesis deployment, the short- and long-axis views of TEE were used to assess the presence of AR and its severity and sites (origins of leak). The severity of AR was assessed qualitatively using color Doppler flow imaging and the maximal jet width at its origin from the prosthesis.[11] AR was graded as follows: 0, absent; 1, trace and mild; 2, mild-to-moderate; 3, moderate-to-severe; and 4, severe.[7,12] In addition, AR was classified as paravalvular or intravalvular, or both. To determine the exact site of origin of paravalvular AR, a short-axis view (30° to 60°) at the level of the proximal (ventricular) end of the implanted prosthesis was used. Accordingly, 6 sites of paravalvular AR were identified using the interatrial septum as a landmark, which helped to identify the noncoronary cusp (Figure 2).

Continuous variables are presented as the mean ± SD or SEM and categorical variables as percentages. Comparisons between patients with and without paravalvular AR after TAVI were performed using unpaired Student's *t* tests (for continuous variables) and the chi-square or Fisher exact test (for categorical variables). To relate the locations of AVC with the sites of paravalvular AR after TAVI using TEE, the locations of AVC with their respective sites of paravalvular AR were matched. Receiver operating characteristic curves were subsequently generated to evaluate the predictive value of the AVC volume in determining paravalvular AR at a specific site. All statistical analyses were performed with the Statistical Package for Social Sciences, version 16.0 (SPSS, Chicago, Illinois). A p value <0.05 was considered statistically significant.

Results

The baseline clinical and echocardiographic characteristics of the study population are presented in Tables 1 and 2. The transfemoral approach was performed in 36 patients

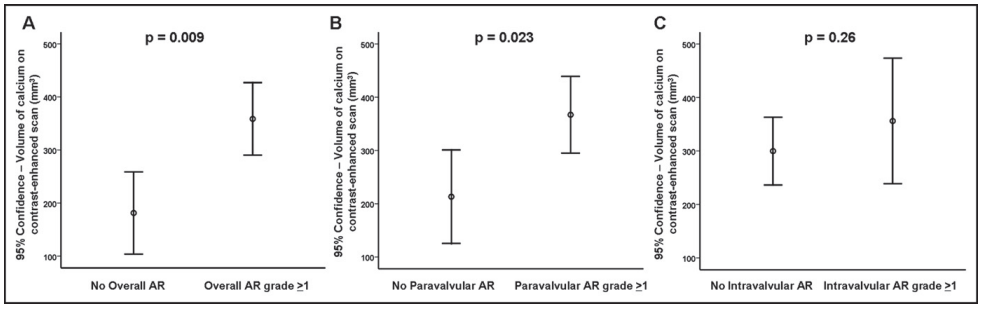

Figure 3. Total volume of baseline AVC on contrast-enhanced multidetector row computed tomographic scans for presence or absence of each type of AR: *(A)* overall, *(B)* paravalvular, and *(C)* intravalvular. Data presented as mean and 95% confidence intervals.

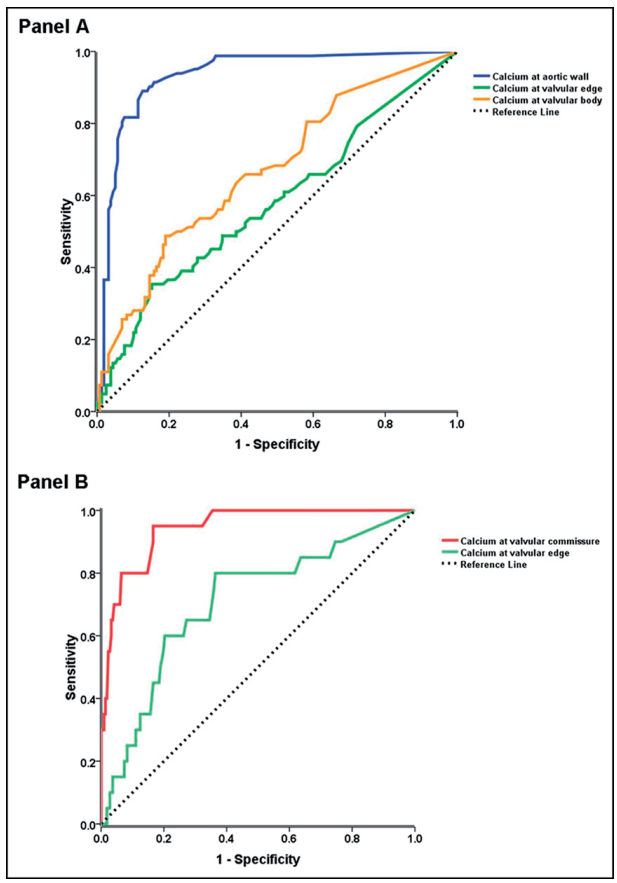

Figure 4. Calcium load and its location as predictor of paravalvular AR at *(A)* aortic wall site or *(B)* commissure site.

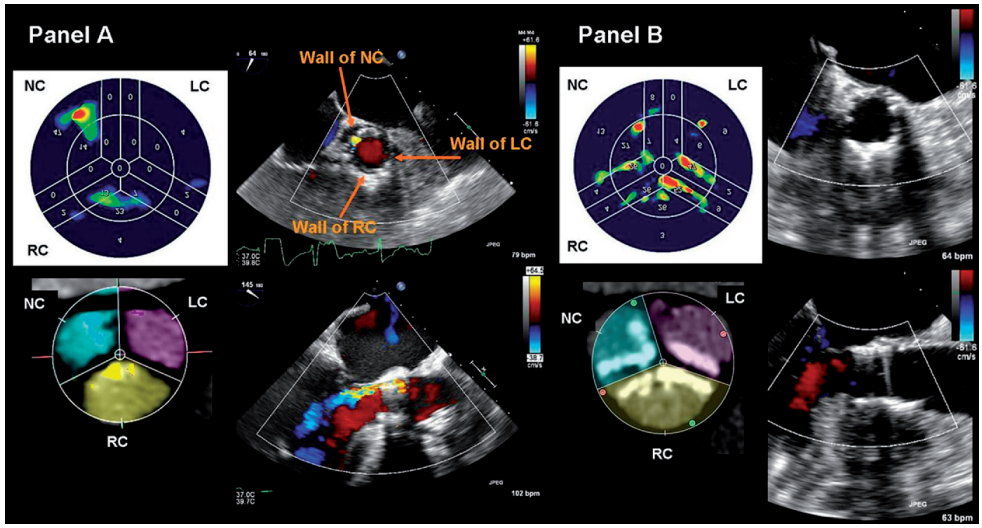

Figure 5. *(A)* Example showing location and volume of AVC on contrast-enhanced multidetector row computed tomographic scan, as provided by automated postprocessing software and subsequent development of paravalvular regurgitation after TAVI. *(B)* Example of patient without paravalvular regurgitation after TAVI showing location and volume of AVC on contrast-enhanced multidetector row computed tomographic scan at baseline. Images of MDCT are rotated for easy comparison with corresponding views on transesophageal echocardiogram. Abbreviations as in Figure 2.

(46%), and the transapical approach in 43. In terms of prosthesis size, 62 patients (78%) received a 26-mm valve and 37 a 23-mm valve. The baseline measurements of the total volume of AVC and volume of calcium on each location of the aortic cusp are listed in Table 3. Because the valvular commissures or valvular free edges were closely related to each other on 2 apposing cusps (Figure 1), they were considered as a unit when AVC was concerned. Hence, the amount of calcium on the valvular commissures or free edges was the summation of their respective volume of calcium on the 2 associated cusps.

Grade 1 or greater AR immediately after initial prosthesis deployment was observed in 63 patients: grade 1 (mild) in 49 (62%), grade 2 (mild-to-moderate) in 11 (14%), and grade 3 (moderate-to-severe) in 1 (4%). The remaining 16 patients (20%) did not have any detectable AR. Severe AR (grade 4) was not observed. In terms of the distribution of AR after TAVI (n = 63), most patients had paravalvular AR (n = 56), and isolated intravalvular AR was observed in a few patients (n = 7). The proportion of patients with and without postprocedural paravalvular AR was comparable among the patients who underwent the transfemoral or transapical approach (45% vs 48% and 55% vs 52%, respectively; p = 0.81) or those who received a 23- or 26-mm prosthesis (21% vs 22% and 79% vs 78%, respectively; p = 1.00).

Among the patients with postprocedural paravalvular AR, 6 potential sites of leakage using TEE in each patient were identified (Figure 2). Hence, the total number of potential sites for the entire population was 474. The prevalence of paravalvular AR at these 6 specified sites is listed in Table 4. The total number of sites with paravalvular AR was 102, and most occurred at the aortic wall sites (82 sites, 80%), with few originating from the valvular commissures (20 sites, 20%).

Patients with a greater AVC volume at baseline had a greater prevalence of AR after TAVI (Figure 3). In particular, the total AVC volume was related to the development of paravalvular AR but not to intravalvular AR after TAVI (Figure 3). Accordingly, the study population was dichotomized into the presence and absence of paravalvular AR to further assess the relation between AVC (and its locations) and the occurrence of paravalvular AR.

To relate the locations of AVC with the presence of paravalvular AR at the 6 specified sites after TAVI, we first matched the locations of AVC with their respective sites of paravalvular AR. For AR originating from the aortic walls (1 from each cusp, 3 sites in total), each AR site was matched with its AVC location on each cusp at the aortic wall, valvular edge, and valvular body, respectively. Next, receiver operating characteristic curves were generated to determine the usefulness of the volume of calcium on its respective AVC location in predicting the presence of paravalvular AR (originating from the aortic wall site). As demonstrated in Figure 4, calcium at the aortic wall had the largest area under the curve (0.93, p <0.001) in predicting the occurrence of paravalvular AR (at the aortic wall site)

compared to calcium at the valvular edge or body (area under the curve 0.58 and 0.67, respectively).

Similarly, for AR originating from the commissures (3 sites in total), each site was matched with its corresponding AVC location on the valvular commissure and the respective valvular edge involved: the left–right, left–noncoronary, and right–noncoronary, respectively. Figure 4 shows that calcium at the valvular commissure had a greater area under the curve than calcium at the valvular edge (0.94 vs 0.71) in predicting the occurrence of paravalvular AR originating from the commissures. Figure 5 shows examples of a grade 1 paravalvular AR and no AR after TAVI and their respective locations and severity of AVC.

Discussion

The present study highlighted that both the amount of calcium and its exact location on the aortic valve are important in determining the development of paravalvular AR after TAVI. The amount of calcium at the aortic wall was the main determinant of subsequent paravalvular AR at the corresponding aortic wall site, and the amount of calcium at the valvular commissure could predict the occurrence of subsequent paravalvular AR, originating from the corresponding commissure.

Previous studies have shown that AVC can be objectively quantified using electron beam computed tomography and MDCT.[13–16] In addition, differing amounts of calcium on the surfaces of the cusps have been observed in excised stenotic aortic valves.[17] Recent studies that focused on the role of AVC and its relation to post-TAVI AR[1,8,13] have been performed using the Agatston score. However, the volumetric calcium scoring method has been shown to improve interscan reproducibility compared with the Agatston score.[9,10,16] Using only unenhanced MDCT, visualization of the valve leaflets can be challenging. Therefore, contrast-enhanced MDCT is commonly performed for better visualization of AVC and its precise location on the aortic valve.[1,2] The present study demonstrated the feasibility of volumetric quantification of AVC, together with its detailed location on the aortic valve, using the automated postprocessing software using contrast-enhanced MDCT.

Although dramatic improvement has occurred in the periprocedural complication rate in the recent TAVI series,[18–20] there is still a significant proportion of patients (72% to 84%) with at least some degree of paravalvular AR after TAVI.[18,21] This is consistent with the results of the present study, which showed that 71% of patients had paravalvular AR. The long-term effect of AR, however mild it might be, is yet to be determined. A few recent studies have alluded to the importance of AVC severity in the development of AR after TAVI.[1,2,8] In a recent study of 57 patients who underwent TAVI (balloon-expandable valves in 33% and self-expanding valves in 67%), Koos et al[2] showed that the severity of AR after deployment was positively related to AVC severity. In addition, John et al[1] demonstrated in 100 patients with self-expanding valve implantation that although a significant relation exists between total calcium at the device landing zone and the grade of paravalvular AR after deployment, this relation was weak ($r = 0.33$, $p = 0.001$). Therefore, the study by John et al[1] suggested that the location of AVC might be more important than the total amount of AVC in determining AR after TAVI.

In the present study, we have confirmed the relation between the location of AVC and the presence of paravalvular AR, the predominant type of AR observed after TAVI. More importantly, we have shown that the main determinant of any detectable paravalvular AR, originating from the aortic wall site, was the amount of calcium at the corresponding aortic wall. Calcium at other locations such as the valvular edge or body was less important in determining the presence of paravalvular AR arising from the aortic wall site. When paravalvular AR originating from the commissure was analyzed, the main determinant of any detectable AR was the amount of calcium at the corresponding commissure of the native valve. Therefore, the results of the present study have highlighted the important role of both the AVC load and its location, in predicting the development of paravalvular leakage after TAVI. Although the mechanism is not entirely clear, the most likely explanation is that the calcified, native aortic valve is pushed outward toward the walls of the aorta initially during ballooning and later, by the balloon expandable bioprosthesis (which has a height of 14 to 16 mm).[22] Therefore, when a significant amount of calcium is present at the circumference of the native valve, it can potentially prevent perfect apposition between the prosthesis and aortic walls and, thus, result in paravalvular AR at these sites. These results suggest that extra caution should be given to patients, particularly those with calcium at the circumference of the native aortic annulus, and perhaps, additional maneuvers such as prolonged ballooning or reballooning might be necessary when paravalvular AR is present after deployment.

We acknowledged that this was a relatively small study and that it was insufficient to study the clinical end points of at least moderate AR after TAVI. This will need to be explored in a larger population.

1. John D, Buellesfeld L, Yuecel S, Mueller R, Latsios G, Beucher H, Gerckens U, Grube E. Correlation of device landing zone calcification and acute procedural success in patients undergoing transcatheter aortic valve implantations with the self-expanding CoreValve prosthesis. *JACC Cardiovasc Interv* 2010;3:233–243.
2. Koos R, Mahnken AH, Dohmen G, Brehmer K, Günther RW, Autschbach R, Marx N, Hoffmann R. Association of aortic valve calcification severity with the degree of aortic regurgitation after transcatheter aortic valve implantation. *Int J Cardiol* 2010;150:142–145.
3. Vahanian A, Alfieri O, Al-Attar N, Antunes M, Bax J, Cormier B, Cribier A, De Jaegere P, Fournial G, Kappetein AP, Kovac J, Ludgate S, Maisano F, Moat N, Mohr F, Nataf P, Piérard L, Pomar JL, Schofer J, Tornos P, Tuzcu M, van Hout B, Von Segesser LK, Walther T; European Association of Cardio-Thoracic Surgery, European Society of Cardiology, European Association of Percutaneous Cardiovascular Interventions. Transcatheter valve implantation for patients with aortic stenosis: a position statement from the European Association of Cardio-Thoracic Surgery (EACTS) and the European Society of Cardiology (ESC), in collaboration with the European Association of Percutaneous cardiovascular Interventions (EAPCI). *Eur Heart J* 2008; 29:1463–1470.
4. Lang RM, Bierig M, Devereux RB, Flachskampf FA, Foster E, Pellikka PA, Picard MH, Roman MJ, Seward J, Shanewise JS, Solomon SD, Spencer KT, St John Sutton MS, Stewart WJ; Chamber Quantification Writing Group, American Society of Echocardiography's Guidelines and Standards Committee, European Association of Echocardiography. Recommendations for chamber quantification: a report from the American Society of Echocardiography's Guidelines and Standards Committee and the Chamber Quantification Writing Group,

developed in conjunction with the European Association of Echocardiography, a branch of the European Society of Cardiology. *J Am Soc Echocardiogr* 2005;18:1440–1463.
5. Baumgartner H, Hung J, Bermejo J, Chambers JB, Evangelista A, Griffin BP, Iung B, Otto CM, Pellikka PA, Quiñones M; EAE/ASE. Echocardiographic assessment of valve stenosis: EAE/ASE recommendations for clinical practice. *Eur J Echocardiogr* 2009;10:1–25.
6. Otto CM. Valvular aortic stenosis: disease severity and timing of intervention. *J Am Coll Cardiol* 2006;47:2141–2151.
7. Zoghbi WA, Enriquez-Sarano M, Foster E, Grayburn PA, Kraft CD, Levine RA, Nihoyannopoulos P, Otto CM, Quinones MA, Rakowski H, Stewart WJ, Waggoner A, Weissman NJ; American Society of Echocardiography. Recommendations for evaluation of the severity of native valvular regurgitation with two-dimensional and Doppler echocardiography. *J Am Soc Echocardiogr* 2003;16:777–802.
8. Delgado V, Ng AC, Van de Veire NR, van der Kley F, Schuijf JD, Tops LF, de Weger A, Tavilla G, de Roos A, Kroft LJ, Schalij MJ, Bax JJ. Transcatheter aortic valve implantation: role of multi-detector row computed tomography to evaluate prosthesis positioning and deployment in relation to valve function. *Eur Heart J* 2010;31:1114–1123.
9. Callister TQ, Cooil B, Raya SP, Lippolis NJ, Russo DJ, Raggi P. Coronary artery disease: improved reproducibility of calcium scoring with an electron-beam CT volumetric method. *Radiology* 1998;208:807–814.
10. Ohnesorge B, Flohr T, Fischbach R, Kopp AF, Knez A, Schröder S, Schöpf UJ, Crispin A, Klotz E, Reiser MF, Becker CR. Reproducibility of coronary calcium quantification in repeat examinations with retrospectively ECG-gated multisection spiral CT. *Eur Radiol* 2002;12:1532–1540.
11. Moss RR, Ivens E, Pasupati S, Humphries K, Thompson CR, Munt B, Sinhal A, Webb JG. Role of echocardiography in percutaneous aortic valve implantation. *J Am Coll Cardiol Imaging* 2008;1:15–24.
12. Detaint D, Lepage L, Himbert D, Brochet E, Messika-Zeitoun D, Iung B, Vahanian A. Determinants of significant paravalvular regurgitation after transcatheter aortic valve implantation: impact of device and annulus discongruence. *J Am Coll Cardiol Imaging* 2009;2:821–827.
13. Koos R, Mahnken AH, Sinha AM, Wildberger JE, Hoffmann R, Kühl HP. Preliminary experience in the assessment of aortic valve calcification by ECG-gated multislice spiral computed tomography. *Int J Cardiol* 2005;102:195–200.
14. Messika-Zeitoun D, Aubry MC, Detaint D, Bielak LF, Peyser PA, Sheedy PF, Turner ST, Breen JF, Scott C, Tajik AJ, Enriquez-Sarano M. Evaluation and clinical implications of aortic valve calcification measured by electron-beam computed tomography. *Circulation* 2004;110:356–362.
15. Budoff MJ, Mao S, Takasu J, Shavelle DM, Zhao XQ, O'Brien KD. Reproducibility of electron-beam CT measures of aortic valve calcification. *Acad Radiol* 2002;9:1122–1127.
16. Morgan-Hughes GJ, Owens PE, Roobottom CA, Marshall AJ. Three dimensional volume quantification of aortic valve calcification using multislice computed tomography. *Heart* 2003;89:1191–1194.
17. Roberts WC, Ko JM. Weights of individual cusps in operatively-excised stenotic three-cuspid aortic valves. *Am J Cardiol* 2004;94:681–684.
18. Rodés-Cabau J, Webb JG, Cheung A, Ye J, Dumont E, Feindel CM, Osten M, Natarajan MK, Velianou JL, Martucci G, DeVarennes B, Chisholm R, Peterson MD, Lichtenstein SV, Nietlispach F, Doyle D, DeLarochellière R, Teoh K, Chu V, Dancea A, Lachapelle K, Cheema A, Latter D, Horlick E. Transcatheter aortic valve implantation for the treatment of severe symptomatic aortic stenosis in patients at very high or prohibitive surgical risk: acute and late outcomes of the multicenter Canadian experience. *J Am Coll Cardiol* 2010;55:1080–1090.
19. Thomas M, Schymik G, Walther T, Himbert D, Lefèvre T, Treede H, Eggebrecht H, Rubino P, Michev I, Lange R, Anderson WN, Wendler O. Thirty-day results of the SAPIEN aortic bioprosthesis European outcome (SOURCE) registry: a European registry of transcatheter aortic valve implantation using the Edwards SAPIEN valve. *Circulation* 2010;122:62–69.
20. Webb JG, Altwegg L, Boone RH, Cheung A, Ye J, Lichtenstein S, Lee M, Masson JB, Thompson C, Moss R, Carere R, Munt B, Nietlispach F, Humphries K. Transcatheter aortic valve implantation: impact on clinical and valve-related outcomes. *Circulation* 2009;119:3009–3016.
21. Zahn R, Gerckens U, Grube E, Linke A, Sievert H, Eggebrecht H, Hambrecht R, Sack S, Hauptmann KE, Richardt G, Figulla HR, Senges J; German Transcatheter Aortic Valve Interventions-Registry Investigators. Transcatheter aortic valve implantation: first results from a multi-centre real-world registry. *Eur Heart J* 2011;32:198–204.
22. Webb JG, Chandavimol M, Thompson CR, Ricci DR, Carere RG, Munt BI, Buller CE, Pasupati S, Lichtenstein S. Percutaneous aortic valve implantation retrograde from the femoral artery. *Circulation* 2006;113:842–850.